Zeitschrift: Schweizerische mineralogische und petrographische Mitteilungen = Bulletin suisse de minéralogie et pétrographie

Band: 57 (1977)

Heft: 1

Artikel: A refinement of the method of plagioclase determination in the zone normal to (010) and (001)

Autor: Bruni, Paolo

DOI: https://doi.org/10.5169/seals-44421

Schweiz. mineral. petrogr. Mitt. 57, 31–40, 1977

A Refinement of the Method of Plagioclase Determination in the Zone Normal to (010) and (001)

By *Paolo Bruni* (Trieste)*)

Abstract

On the basis of available optical data of low-T and high-T plagioclases (Burri et al., 1967), diagrams representing the extinction angles in zones ⊥ (010) and (001) are presented. For any initial value of 2V, a variation from $-10°$ to $+10°$ has been considered in order to show the relation between the actual 2V and the greatest extinction angles.

The following work is concerned with plagioclases twinned according to the Albite and Manebach laws and with untwinned individuals. It is to complete an earlier study (Bruni, 1976) dealing with plagioclases twinned according to the Carlsbad, Albite-Carlsbad, Ala B, Albite-Ala B, Ala A, Manebach-Ala A laws.

The diagrams of figs. 1–4 represent the extinction angles in zones ⊥ (010) and (001). They are valid only if there is a perfect correspondence between the actual 2V and the 2V adopted by Burri et al. (1967); otherwise the actual curves will differ more or less widely from the curves represented here.

The diagrams of figs. 5–8 represent the greatest extinction angles in zones ⊥ (010) and (001). They are valid both for 2V values adopted by the above mentioned authors (dotted lines), and for any 2V value deviating from them by up to $\pm 10°$. The curves in these diagrams represent points of the plane having the same $2V_\gamma$ (marked on each line).

Considering the greatest extinction angles in zone ⊥ (010), one can recognize that even a great variation of 2V exerts only a small influence upon the determination of An up to values of 65–70%. However, for greater An contents than 70%, errors which can exceed even 15% may result. For example, an extinction angle of 52.5° for high-T plagioclases corresponds to 86% An if $2V_\gamma$ is equal to 98°; but such an extinction angle could correspond both to a plagioclase with 80% An and $2V_\gamma$ equal to 90°, and to a plagioclase with 94% An and $2V_\gamma$ equal to 110°.

*) Istituto di Mineralogia e Petrografia, Piazzale Europa 1, I-34100 Trieste.

To avoid this imprecision of An determination, it is necessary to compare a measurement of the greatest extinction angle in zone ⊥ (010) with another measurement in zone ⊥ (001): in such a way, these two extinction angles would determine the same pairs of 2V, An values. For example, a greatest extinction angle of 50° measured in zone ⊥ (010) for a high-T plagioclase and an angle of 44.9° in zone ⊥ (001) refers only to a value of 85% An, which is the value corresponding to the same $2V_{\gamma}$ (105°) on both diagrams. Hence, only by the presence of both planes (010) and (001) can one remove the uncertainty arising in the determination of An content of the very Ca-rich plagioclases.

Bibliography

BRUNI, P. (1976): Plagioclase determination through measurement of the extinction angles in sections normal to (010) and (001). SMPM 56, 39–54.

BURRI, C., R. L. PARKER und E. WENK (1967): Die optische Orientierung der Plagioklase. Basel, Birkhäuser.

Manuscript received November 11, 1976.

Legend of Figures:

λ: angle between observation direction and c-axis or a-axis (variation curves in zone ⊥ (010) and (001), respectively).

Ext.: extinction angles.

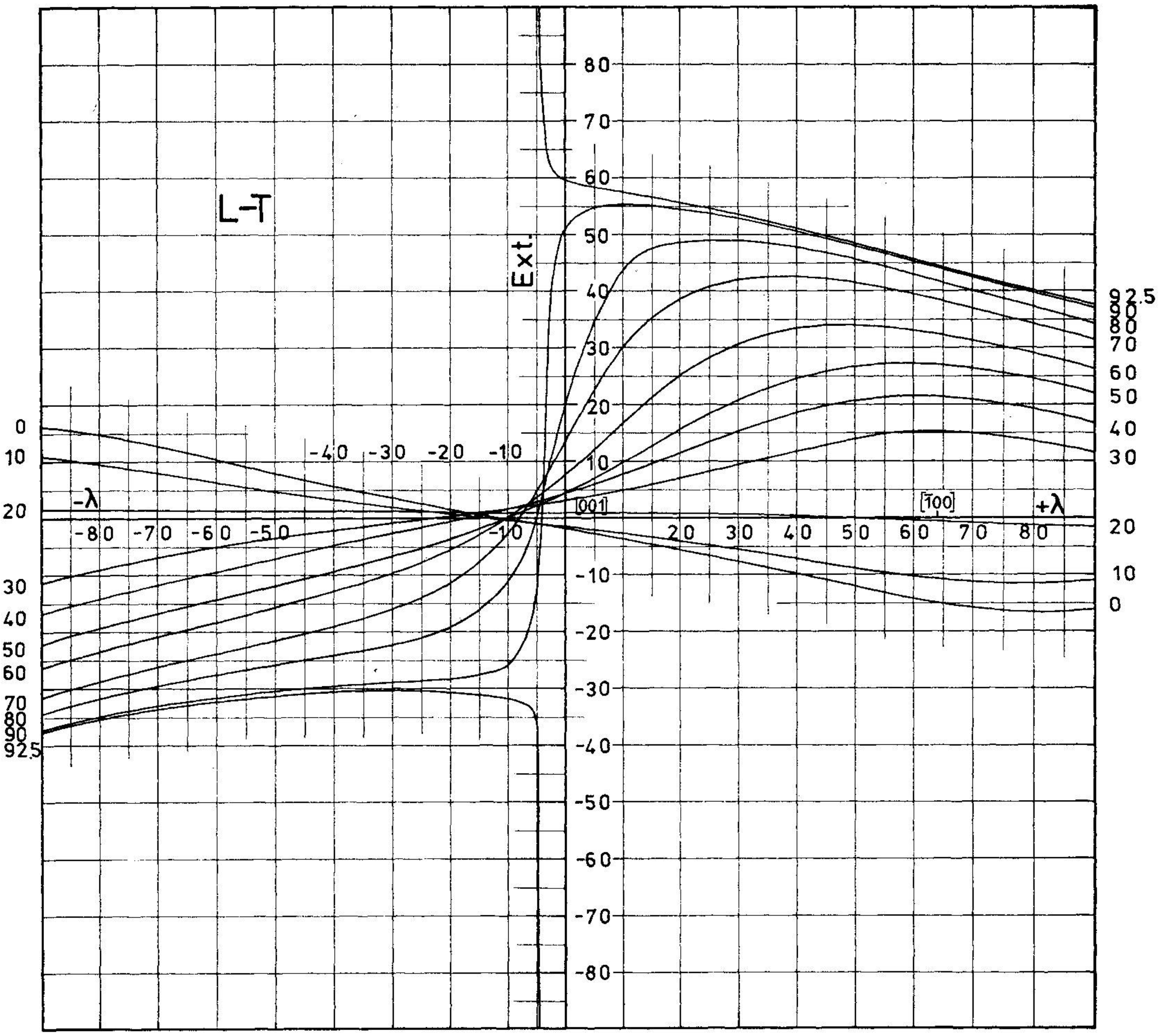

Fig. 1. Extinction angles $n_\alpha' \wedge (010)$ in zone $\perp$ (010) of low-T plagioclases.

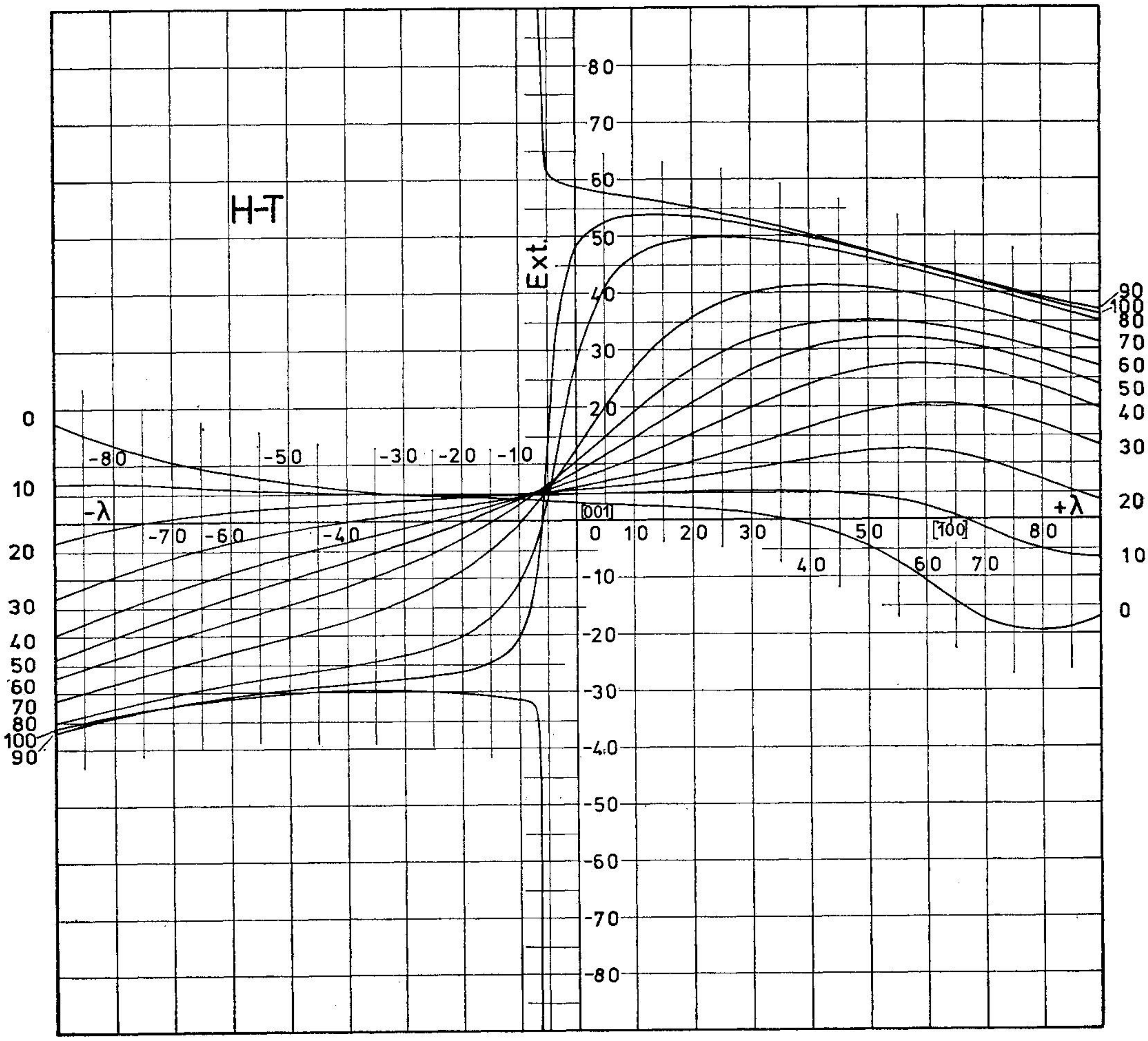

Fig. 2. Extinction angles $n_{\alpha}' \wedge (010)$ in zone $\perp$ (010) of high-T plagioclases.

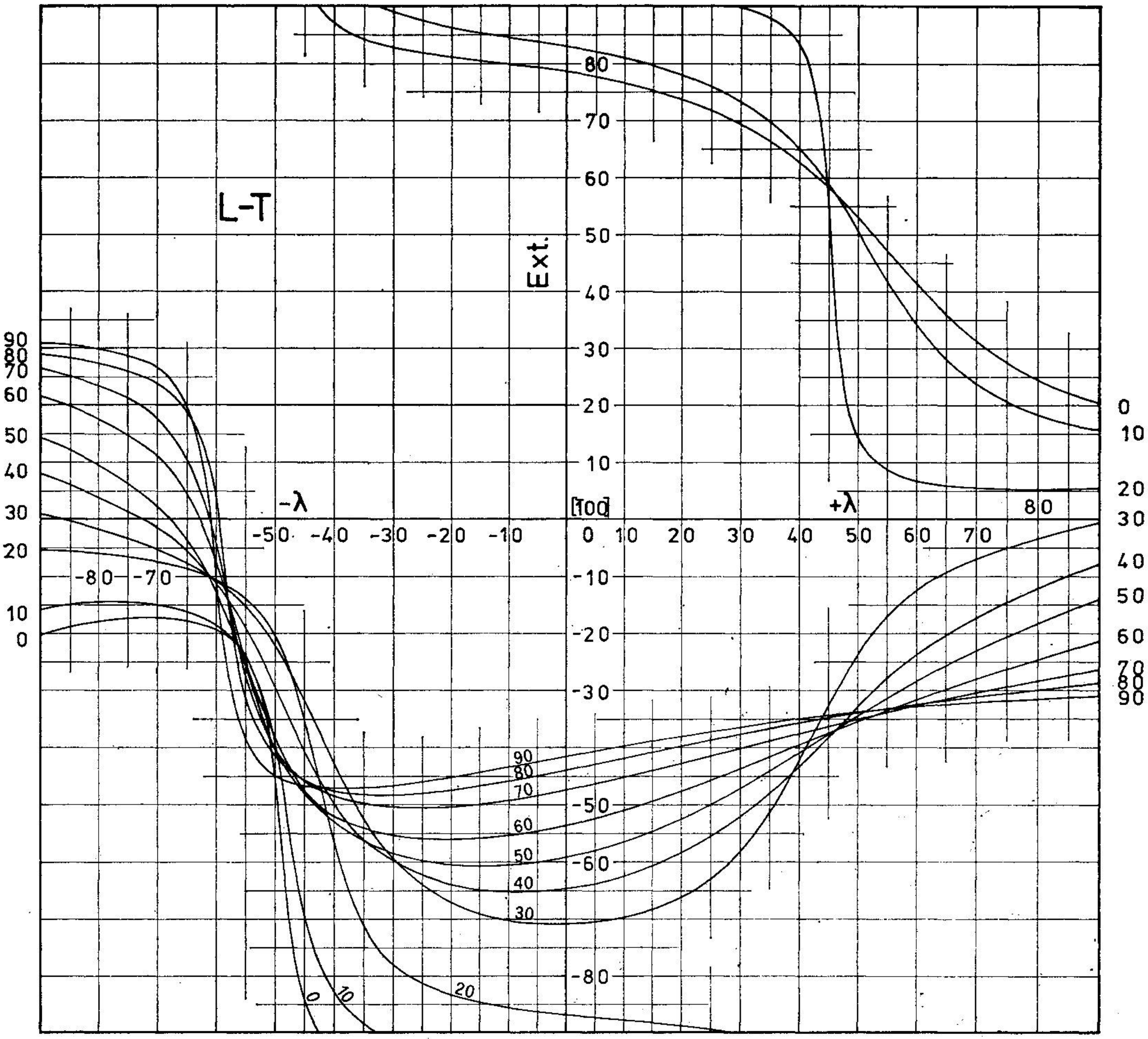

Fig. 3. Extinction angles $n_{\alpha}' \wedge (001)$ in zone $\perp$ (001) of low-T plagioclases.

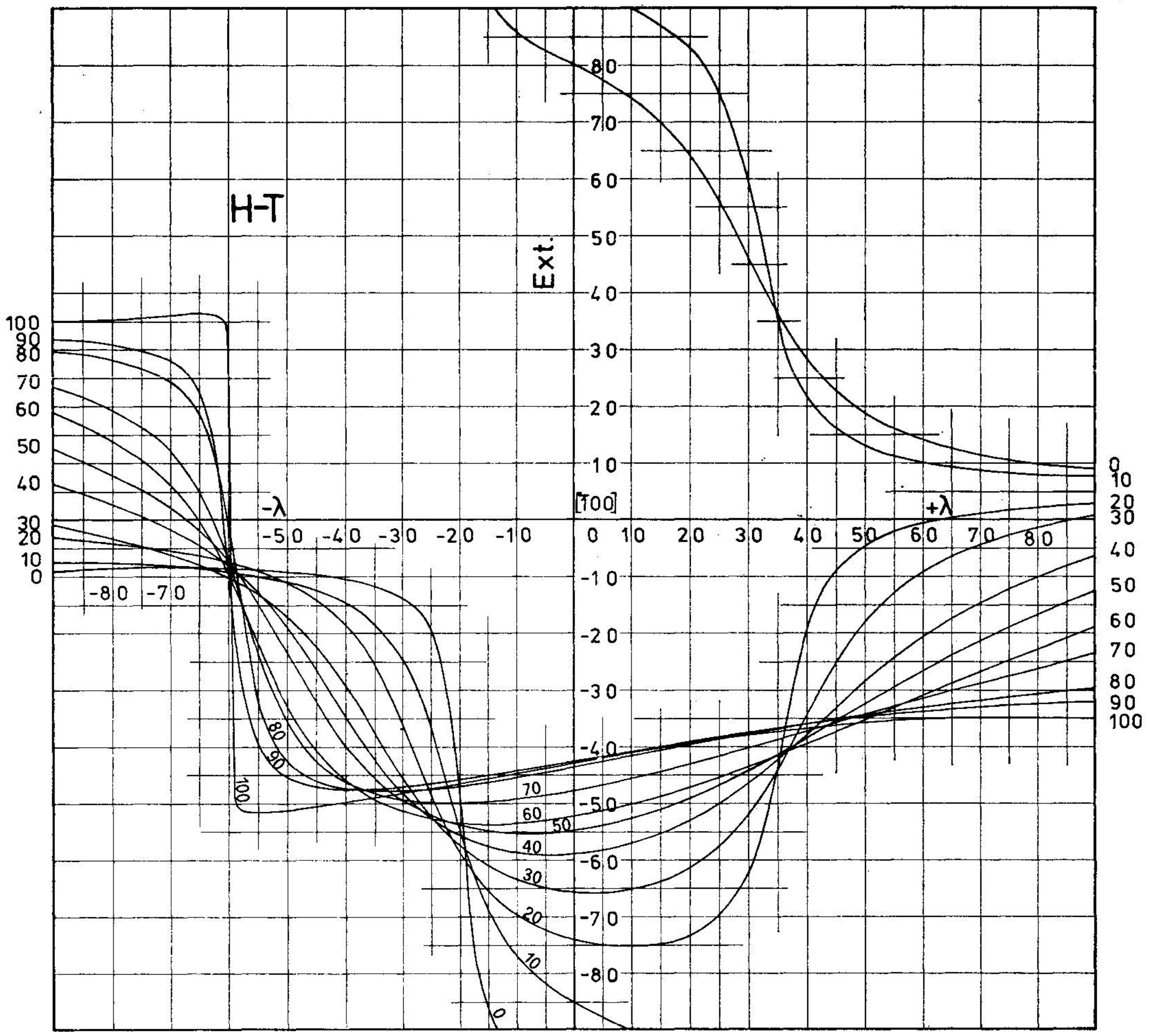

Fig. 4. Extinction angles $n_{\alpha}' \wedge (001)$ in zone $\perp$ (001) of high-T plagioclases.

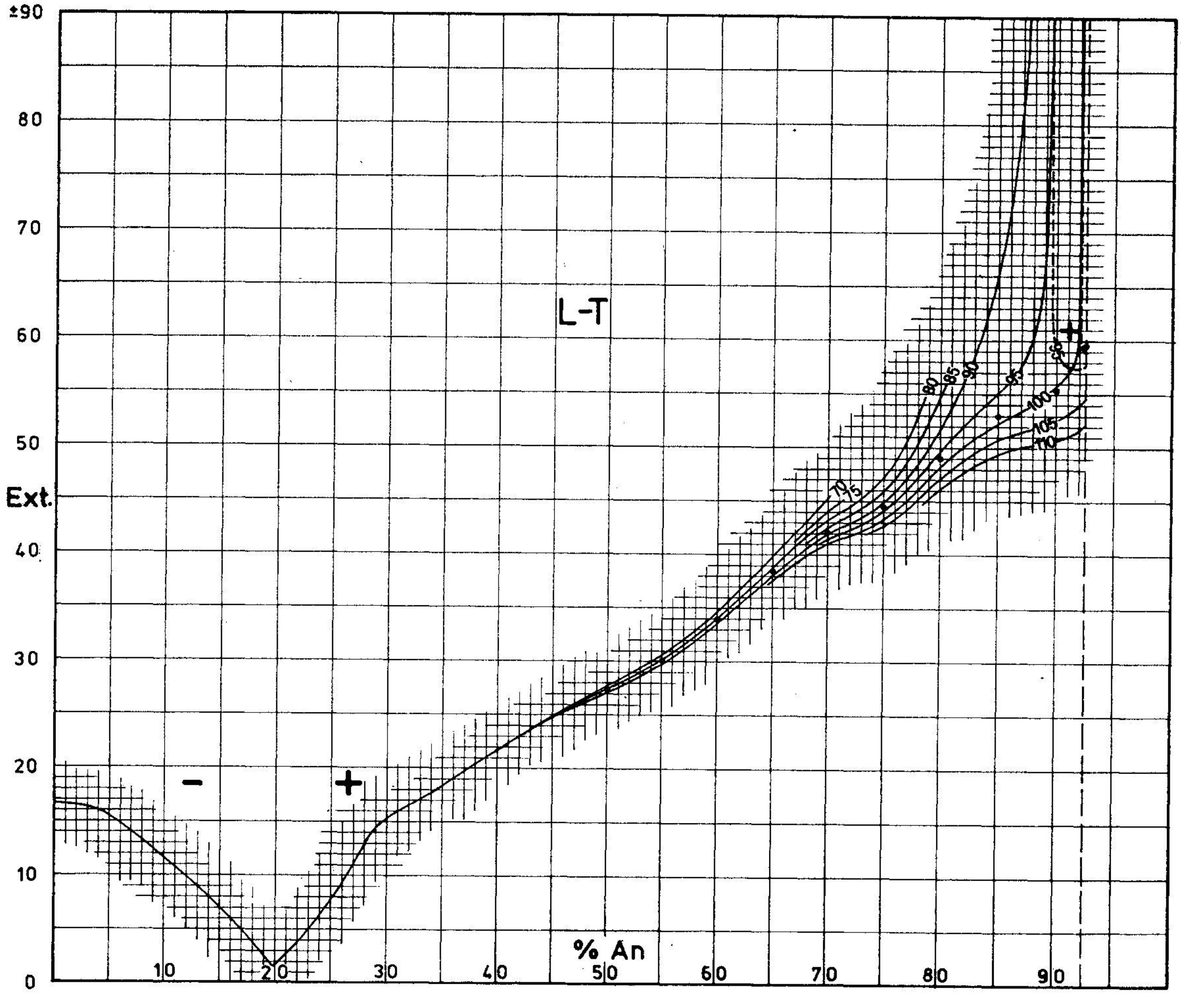

Fig. 5. Greatest extinction angles $n_{\alpha}' \wedge (010)$ (full lines) and $n_{\gamma}' \wedge (010)$ (hatched lines) in zone $\perp$ (010) of low-T plagioclases. For explanation see text.

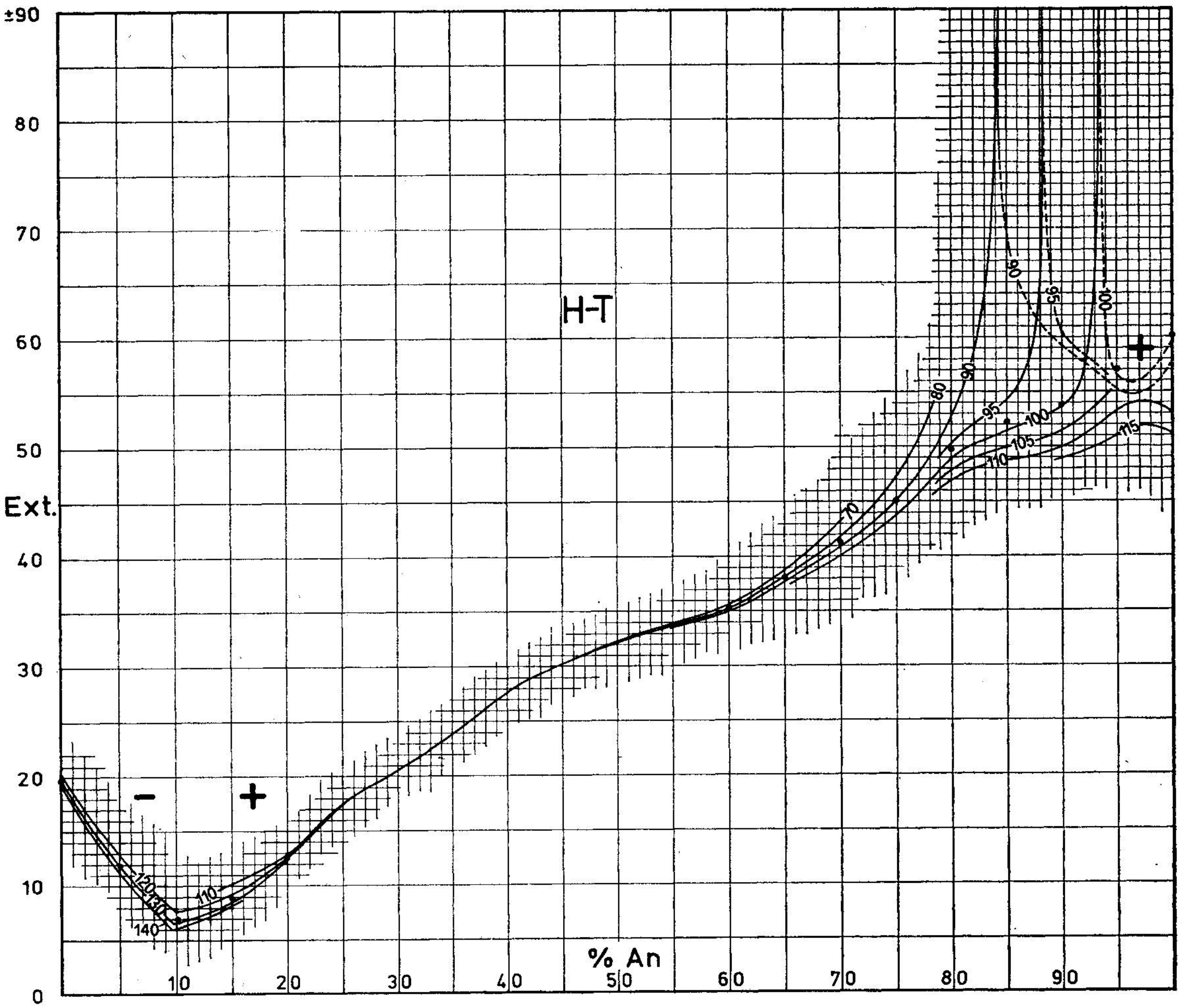

Fig. 6. Greatest extinction angles $n_{\alpha}' \wedge (010)$ (full lines) and $n_{\gamma}' \wedge (010)$ (hatched lines) in zone $\perp$ (010) of high-T plagioclases. For explanation see text.

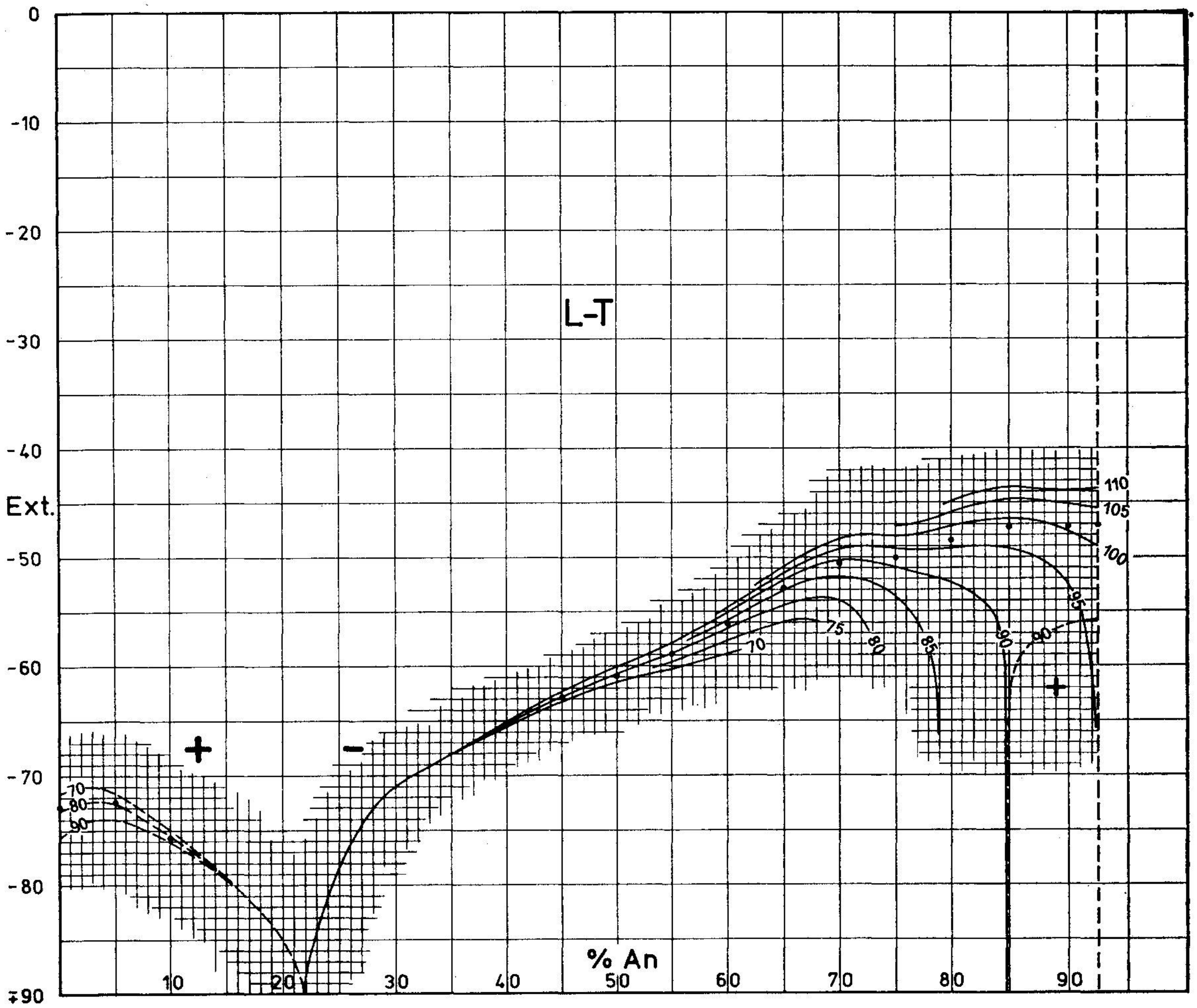

Fig. 7. Greatest extinction angles $n_\alpha' \wedge (001)$ (full lines) and $n_\gamma' \wedge (001)$ (hatched lines) in zone ⊥ (001) of low-T plagioclases. For explanation see text.

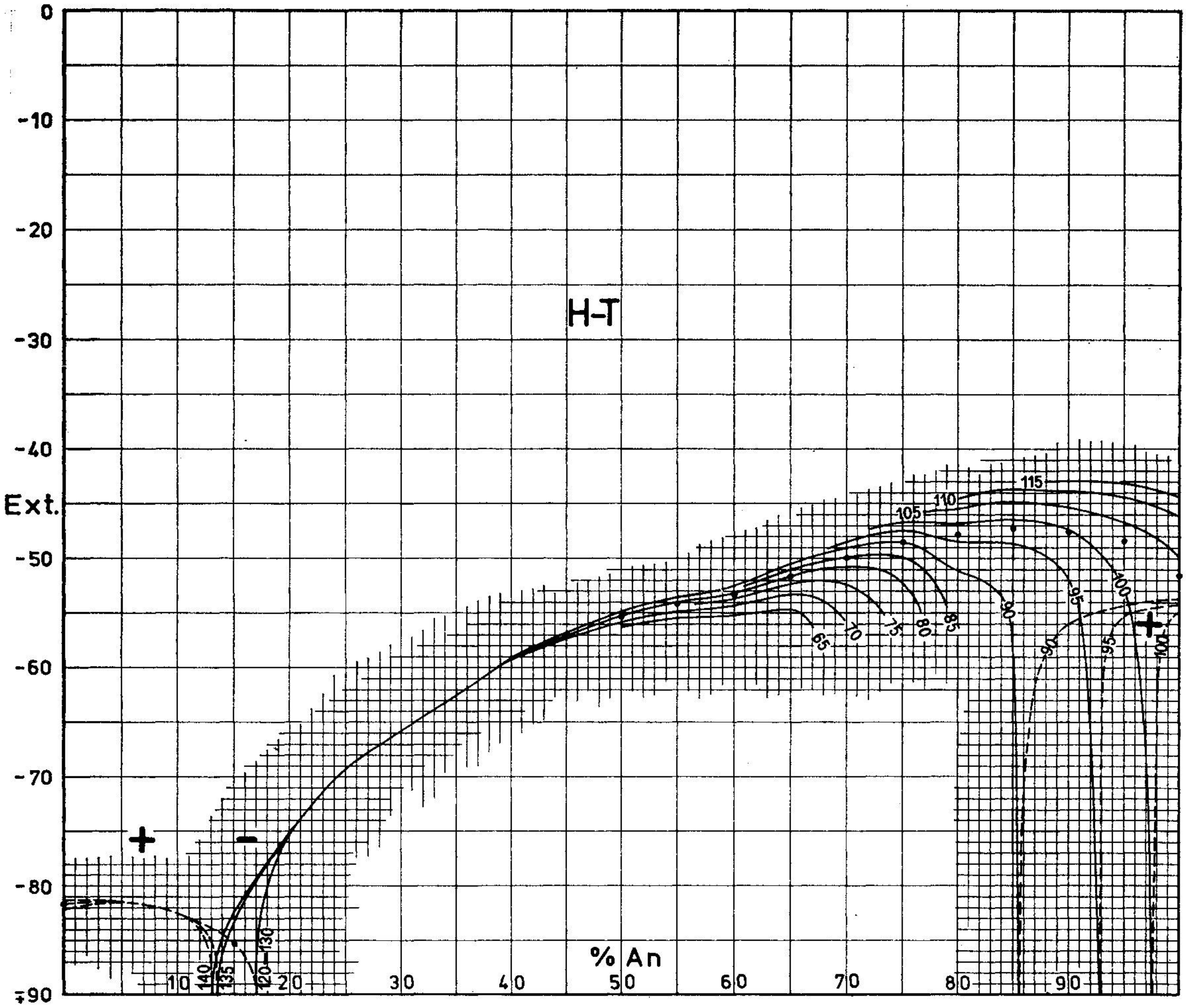

Fig. 8. Greatest extinction angles $n_{\alpha}' \wedge (001)$ (full lines) and $n_{\gamma}' \wedge (001)$ (hatched lines) in zone $\perp$ (001) of high-T plagioclases. For explanation see text.